Uniosun Journal of Engineering and Environmental Sciences (UJEES), Vol. 8 No. 2, Sept., 2026
DOI: 10.64980/ujees.v8i2.020 **Amole et al.**
Published: September 30, 2026

AN EXPLORATORY STUDY OF SELECTED ENERGY STORAGE SYSTEM UNDER DIFFERENT LOAD MODELS CONSIDERING TECHNICAL AND ECONOMIC METRICS

Abraham O. AMOLE[1*], Hafsoh K. OGUNNIYI[2], Idris A. TIJANI[3], Desmond E. IGHRAVWE[4], Oluwaseun A. BAMIDO[5], Ignatius K. OKAKWU[6]

[1,2,3,5]Department of Electrical/Electronics and Telecommunications Engineering, Bells University of Technology, Ota, Ogun State, Nigeria
[4]Department of Mechanical Engineering, Bells University of Technology, Ota, Ogun State, Nigeria
[6]Department of Electrical and Electronics Engineering, Olabisi Onabanjo University, Ago-Iwoye, Ogun State, Nigeria.

[*]Corresponding Author: aoamole@bellsuniversity.edu.ng

Abstract
Energy storage systems (ESS) plays a pivotal role in reliable and sustainable operation of renewable energy systems. However, ESS perform differently under different loading conditions. This study investigated the performance of Flow (F), Lithium-Ion (LI), and Lead-Acid (LA) ESS under residential (RL), commercial (CL), industrial (IL), and community (ComL) load profiles using HOMER software. Performance evaluation was based on storage depletion (SD), Losses, annual throughput (AT), autonomy (Auto), usable storage capacity (USC), total system cost (TSC), and levelized cost of energy (LCOE). The simulation results revealed that FESS possessed the lowest SD of 5.38 kWh/yr under RL while the lowest Losses of 233 kWh/yr was obtained for LIESS under RL. Similarly, the highest AT of 5,586,275 kWh/yr was found in LAESS under IL while the highest USC of 41,751 kWh was recorded in LAESS under IL. Economically, the lowest TSC of $32,318.56 was recorded for FESS under RL and lowest LCOE of $0.5263 for FESS under CL. It can be generally concluded from this study that load type generally impacts the technical, and economic performance of the selected ESS. The study pursues realization of sustainable development goal 7 (SDG 7) as it finds application as a guide in the planning, design, and deployment of renewable energy systems.

Keywords
Energy storage systems, Solar photovoltaic (PV), Lithium-ion storage, Levelized cost of energy, storage depletion

1. INTRODUCTION

An accelerated urbanization and population growth rates as well as the pressing need to decarbonize energy sector is fundamentally reshaping the global energy landscape. By 2040, global energy demand is expected to rise by about 33% [1], and renewable energy's share of the global electricity mix is projected to exceed 62% by 2050, with solar PV accounting for the largest percent [2]. With the cost of solar PV modules decreasing and the conversion efficiency steadily improving, solar PV has become the fastest-growing renewable technology in recent years [3]. This increasing trend is hindered by the variable and intermittent nature of solar PV generation, which strongly relies on meteorological conditions and daily cycles [4]. The variability of renewable resources often cause a basic imbalance between energy supply and demand, leading to energy deficit, excess power generation curtailment, and suboptimal energy use [5][6]. To address this challenge, a key solution is the adoption of energy storage systems (ESS), which offer the characteristics of high energy density, modularity, and fast charge/discharge cycles, ensuring high efficiency in fast response energy buffering and load-shifting, as well as improving grid reliability [7].

Various energy storage systems (ESS) are already in the market each with distinct electrochemical features for energy storage use. Lithium-ion energy storage systems (LIESS) are commonly used because they are characterized by highest energy density ranging between 75 – 250 Wh/kg, high round-trip efficiency between 85 – 95%, and are becoming more cost effective [8], [9], [10]. Consequently, there are a number of literatures considering various dimensions of LIESS [11], [12], [13]. Despite its less favorable cycle-life and depth-of-discharge limitations, Lead-Acid energy storage systems (LAEES) continue to be relevant in the cost-sensitive, small-scale off-grid market due to their well-established technology base and low initial capital expenditure ranging between $50–400/kWh [15], [16]. The flow energy storage systems (FESS) among which includes Vanadium Redox Flow Batteries (VRFB) have the remarkable property of separating power and energy ratings

characteristics. They are characterised by exceptional cycle durability of above 10,000 cycles and negligible capacity degradation, particularly suited for high-throughput and long-duration storage applications [17], [18]. One of the most important yet often underestimated aspects of ESS implementation is the selection of the ESS to match the requirements of various load profiles. Though there are substantive studies on the subject of ESS selection however, they are mainly based on manufacturer-supplied specifications or cost minimisation heuristics that do not sufficiently consider the compatibility of the ESS electrochemical characteristics and the temporal demand profiles of specific loads [19], [20]. The practical implications of inappropriate ESS selection is that it may suffer reduced operational time over a relatively short period of operation due to the degradation of ESS resulting from suboptimal battery-load pairing [7].

Currently, only limited literatures focused on comprehensive comparative assessment of various ESS performance under various load profile types. The majority of current investigations are either ESS characterisation studies [21], [22] or single-application economic optimisation [23], [24], [25] that lacks correlation between ESS technology-specific performance properties and application-specific deployment requirements. This limitation often hinders energy system planners, system designers, and renewable energy system developers from making decisions based on realistic evidence. To address this gap, the present study proposes a comprehensive simulation-based comparative assessment of FESS, LIESS and LAESS in standalone solar PV energy systems for residential, commercial, industrial and community load profiles. The novelty of this work is the multi-criteria assessment of different ESS technologies under 4 different load profiles to synthetize the results into an application specific selection framework.

MATERIALS AND METHOD

This study leveraged simulation approach to assess the performance of three namely; Flow (F), Lithium-Ion (LI), and Lead-Acid (LA) energy storage systems (ESSs) under four types of load profiles namely; residential load (RL), commercial load (CL), industrial load (IL), and community load (ComL) in standalone solar PV energy systems as shown in Figure 1. The stages involved include; system design, ESS selection, load profiling, simulation environment, and performance evaluation as discussed in the subsequent subsections.

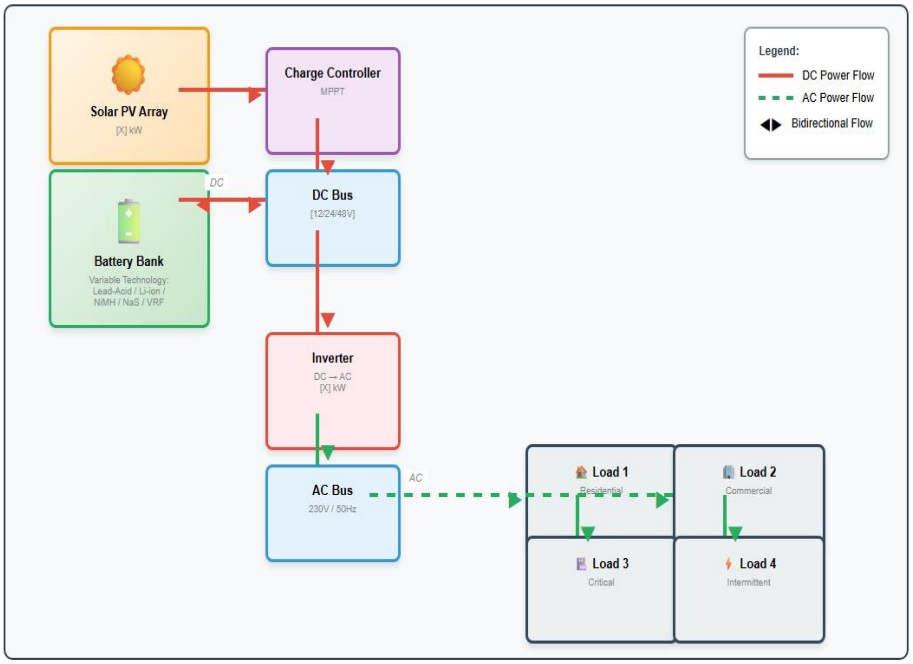


Figure 1: Standalone Solar PV System Schematic

2.1 System design

The solar PV energy system evaluated in this study comprises four principal subsystems. A solar PV array, charge controller, energy storage, and power conversion system (PCS). System sizing was governed by established analytical relationships. The required PV array capacity is expressed in Equation 1 [26]:

$$PPV = \frac{Edaily}{PSH \times \eta system} \quad (1)$$

Where PPV is required PV array capacity (kW), $Edaily$ is average daily energy demand (kWh/day), PSH is peak sun hours (hours/day), $\eta system$ is overall system efficiency ranging between 0.75-0.85. The required storage capacity is expressed in Equation 2 as [27]:

$$\text{Cstorage} = \frac{(\text{Edaily} \times \text{DoDdays})}{(\text{DoDmax} \times \eta\text{battery} \times \text{Vsystem})} \quad (2)$$

Where Cstorage is required storage capacity (Ah), DoDdays is days of autonomy (backup days), DoDmax is maximum permissible depth of discharge, ηbattery is battery efficiency, Vsystem is System voltage (V). The required storage energy capacity is expressed in Equation 3 as [27]:

$$\text{Estorage} = \frac{(\text{Edaily} \times \text{Dautonomy})}{\text{DoDmax}} \quad (3)$$

Where Estorage is the required storage energy capacity (kWh). The storage management system (SMS) monitors state of charge (SoC), temperature, and cell balancing to prevent overcharging and deep discharge, as discussed in Section 2.2. The state of charge is expressed in Equation 4 as [28]:

$$\text{SoC}(t) = \left[\frac{Q(t)}{\text{Qnom}}\right] \times 100\% \quad (4)$$

Where $Q(t)$ is current storage charge at time t (Ah), Qnom is nominal storage capacity (Ah). The SoC changes dynamically based on charging and discharging processes. The dynamic state of charge is expressed in Equation 5 as [29]:

$$\text{SoC}(t+1) = \text{SoC}(t) + \frac{\left[(\eta\text{charge} \times \text{Icharge} \times \Delta t) - \left(\frac{\text{Idischarge} \times \Delta t}{\eta\text{discharge}}\right)\right]}{\text{Qnom}} - \sigma \times \Delta t \quad (5)$$

Where Icharge is charging current (A), Idischarge is discharging current (A), Δt is time step (hours), ηcharge and ηdischarge is the charging and discharging efficiencies, respectively, σ is self-discharge rate (%/hour). The depth of discharge (DoD) represents the percentage of storage capacity discharged as shown in Equation 6 [30]:

$$\text{DoD} = 100\% - \text{SoC} = \left[\frac{(\text{Qnom} - Q(t))}{\text{Qnom}}\right] \times 100\% \quad (6)$$

Power conversion system (PCS) converts stored DC power into alternating current (AC) suitable for the connected load while maintaining power quality. The required PCS capacity is expressed in Equation 7 [31]:

$$P_{PCS} = \left(\frac{\text{Pload,peak}}{\eta\text{inverter}}\right) \times \text{SF} \quad (7)$$

Where P_{PCS} is the required inverter capacity (kW), Pload, peak is peak load power (kW), ηinverter is inverter efficiency typically ranging between 0.90-0.95, and SF is safety factor. The load is modeled using predefined load profiles that capture different demand patterns, including residential, commercial, community, and industrial consumption scenarios.

2.2 Energy storage system selection

This study evaluates the performance of three most deployed ESS in today's stationary energy storage applications namely; Flow (F), Lithium-Ion (LI), and Lead-Acid (LA) ESS.

The FESS store energy in two external electrolyte tanks containing vanadium ions in sulphuric acid solution, and power generation takes place in an electrochemical cell stack by redox couple VO_2^+/V^{2+}. FESS are distinguished by the ability to allow scaling up of power and energy capacity without the loss in capacity due to cross-contamination. They can achieve the full depth of discharge (0-100% SOC) with minimal degradation and have a cycle life of more than 10,000 cycles.

LIESS works in the reversible intercalation of lithium ions (Li^+) between a graphite anode and a lithiated oxide cathode. The overall cell reaction is depicted in Equation 8 [32]:

$$LiC_6 + CoO_2 \rightleftharpoons LiCoO_2 + C_6 \quad (8)$$

The LIESS is characterized by gravimetric energy density ranging between 75–250 Wh/kg, volumetric energy density between 200 – 500 Wh/L, round-trip efficiency between 85 – 95% and cycle life ranging 2,000 – 10,000 cycles depending operating conditions.

LAESS in the double sulphate reaction is presented in Equation 9 [33]:

$$PbO_2 + Pb + 2H_2SO_4 \rightleftharpoons 2PbSO_4 + 2H_2O \quad (9)$$

The LAESS have cycle life ranging 500-2,500 cycles and specific energy ranging 30-50 Wh/kg, and are very sensitive to deep discharge which increases sulphation and capacity fade.

2.3 Load Profiles

A total of four load scenarios namely; residential load (RL), commercial load (CL), industrial load (IL), and community load (ComL) which are representative of various real-world load characteristics were considered in this study for the evaluation of ESSs performance.

RL has a distinct consumption pattern during the day with high levels of demand in the evening between 17:00 and 21:00, and a moderate level in the morning. It has a high day-to-day variability, due to occupant behaviour

and diversity of the load. CL has dominant energy demand during the daytime with low demand at night and during the weekends. CL generally hits 10kW and above with economic drivers prioritising peak demand charge reduction and maximising PV self-consumption.
IL has a high steady energy consumption during periods of operation. ESS is most stressed in industrial applications, specifically with regards to the volume of energy throughput, and the requirement for continuous cycling. ComL represents an aggregated multi-user demand for a localised ESS or microgrid with higher demand variability due to the superimposition of various load patterns. The various load profile used for simulation in this study is presented in Table 1.

Table 1: ComL, CL, IL, and RL Profiles

Hour	ComL (kW)	CL (kW)	IL (kW)	RL (kW)
00:00	30.000	2.000	1,000.000	0.521
01:00	30.000	2.000	1,000.000	0.454
02:00	30.000	2.000	1,000.000	0.454
03:00	30.000	2.000	1,000.000	0.454
04:00	30.000	2.000	1,000.000	1.563
05:00	30.000	3.000	1,000.000	2.390
06:00	30.000	5.000	1,000.000	2.629
07:00	100.000	7.000	1,000.000	2.390
08:00	200.000	8.000	1,000.000	2.008
09:00	200.000	8.000	1,000.000	2.055
10:00	200.000	8.000	1,000.000	2.366
11:00	200.000	8.000	1,000.000	2.548
12:00	200.000	8.000	1,000.000	3.303
13:00	200.000	8.000	1,000.000	2.481
14:00	200.000	8.000	1,000.000	1.998
15:00	200.000	8.000	1,000.000	1.898
16:00	200.000	9.000	1,000.000	1.955
17:00	160.000	10.000	1,000.000	3.145
18:00	130.000	12.000	1,000.000	5.884
19:00	100.000	12.000	1,000.000	4.794
20:00	30.000	12.000	1,000.000	3.231
21:00	30.000	12.000	1,000.000	2.294
22:00	30.000	9.000	1,000.000	1.434
23:00	30.000	5.000	1,000.000	0.975

2.4 Simulation Environment

The simulations were performed with Hybrid Optimization of Multiple Energy Resources (HOMER) Pro, which is a popular microgrid design and optimisation platform. HOMER simulates the hourly time steps for a year to account for seasonal variations in loads and solar irradiance. The HOMER simulation diagrams for CL with all the three ESS are shown in Figure 2. A total of twelve (12) simulation scenarios were created with each of the three (3) ESSs subjected to all the four (4) load profiles in Table 1. The system parameters for LIESS, FESS, and LAESS are presented in Table 2 while the solar resources used in this study is presented in Table 3.

2.5 Performance Evaluation Metrics

To assess the technical performance and economic viability of the ESSs under all the load profiles, ten performance indicators used were defined as follows.

i. *State of charge (SoC)* measured in % indicates the dynamic real-time charge level relative to nominal capacity.

ii. *Storage depletion (SD)* represents complete or critical reduction of stored usable energy. It is a temporary state of empty reserves and not physical battery wear and it is measured in kWh/yr or percentage. It is mathematically expressed as Equation 10

$$SD = \frac{E_m - E_c}{E_m} \times 100 \quad (10)$$

Where E_m is the maximum capacity of the ESS and E_c is the available energy currently in the ESS.

iii. *Losses* indicates the cumulative all resistive, conversion and self-discharge losses are overall system energy conversion efficiency. It is measured in kWh/yr.

iv. *Annual throughput (AT)* measured in kWh/yr is the total energy discharged from the storage in a year. AT represents the energy handling capacity.

v. *Usable storage capacity (USC)* measured in kWh represents the amount of energy capacity that can be discharged based on the constraints imposed by depth-of-discharge.

vi. *Cycle service life (CSL)* estimates the operational lifespan based on accumulated throughput over which was specified in the manufacturer's lifetime throughput.
vii. *Autonomy (Auto)* in hours indicates the time for which the battery is able to meet load demand without the PV generation.
viii. *Storage wear cost (SWC)* $/kWh economic cost of battery degradation per unit of energy throughput.
ix. *Total system cost (TSC)* in $ is an economic indicator which cumulatively measures the battery acquisition cost, replacement costs, and annualised capital cost over system lifetime.
x. *Levelized cost of energy (LCOE)* is the average cost per unit of energy delivered over the system's operating life. It is an important economic comparability measure in $/kWh.

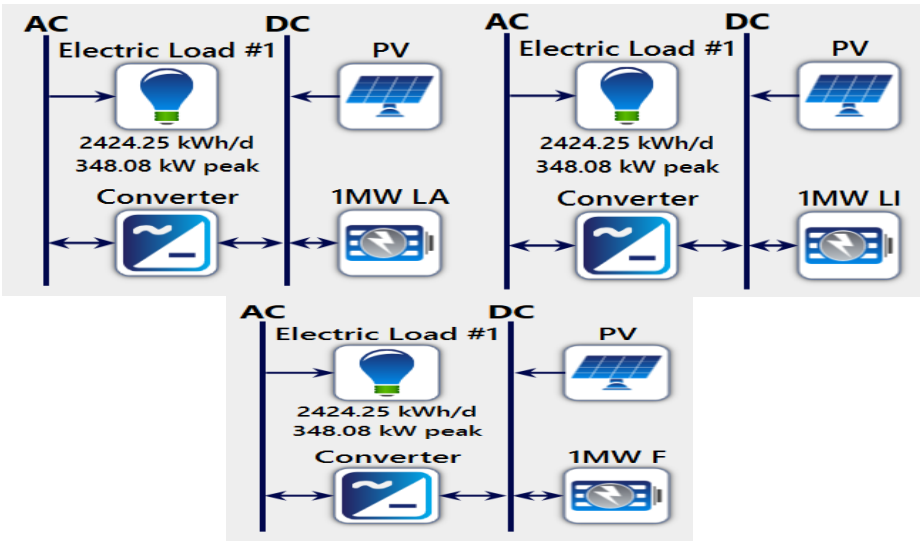


Figure 2: HOMER simulation diagram for CL with LAESS, LIESS, and FESS

Table 2: System parameters for LIESS, FESS, and LAESS

System Parameters	LIESS	FESS	LAESS
ESS size	1 MW	1 MW	1 MW
PV Size	100 kW	100 kW	100 kW
Nominal Voltage	600 V	50 V	12 V
Roundtrip efficiency	90 %		80 %

Table 3: Solar irradiance for the study

Month	Clearness Index	Solar irradiance (kWh/m^2/day)
Jan	0.577	5.810
Feb	0.577	5.990
Mar	0.550	5.780
Apr	0.561	5.720
May	0.588	5.680
Jun	0.623	5.800
Jul	0.621	5.860
Aug	0.592	5.870
Sep	0.574	5.930
Oct	0.587	6.080
Nov	0.581	5.860
Dec	0.581	5.760

3. RESULTS AND DISCUSSION

The results of the scenarios considered in this study under operational, technical, and economic performance is presented and discussed in this section.

3.1 Operational Performance Analysis

Figures 3 -14 shows the SoC and the corresponding frequency for all the twelve scenarios considered in this study. It can be seen from these Figures that both SoC and frequency of the three ESS varied significantly in all the scenarios. In all the scenarios, it was generally observed that ESS were in medium to high SoC ranges between 70-100% with a low occurrence of deep discharge events. These characteristics enhances the ESS lifecycle. It was specifically observed that the SoC cycling of FESS was most dynamic due to intense loading conditions in IL and CL scenarios. FESS SoC was found to range between 80% and 100% for RL resulting

from low energy demand. It can be inferred that LIESS generally exhibit a good and predictable SoC performance for all load profiles with the highest cycling under IL and significant SoC variability under RL. It was also observed that LAESS exhibited a fairly conservative SoC profile with prevalent high SoC ranging between 75–95% for the duration been considered.

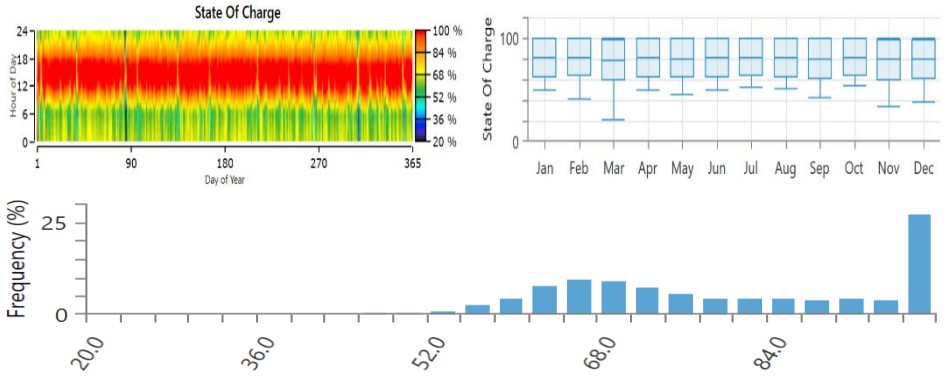


Figure 3: FESS SoC and Frequency for ComL

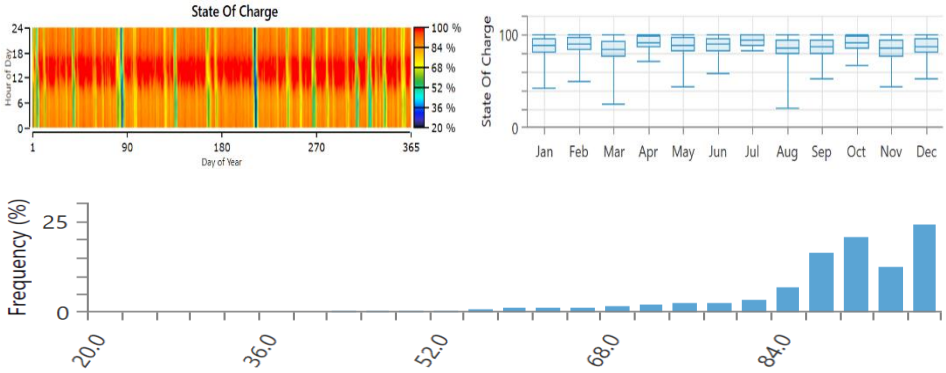


Figure 4: FESS SoC and Frequency for CL

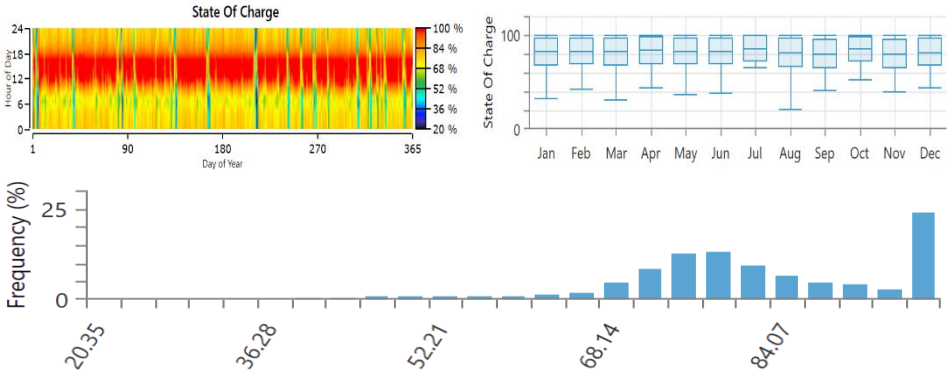


Figure 5: FESS SoC and Frequency for RL

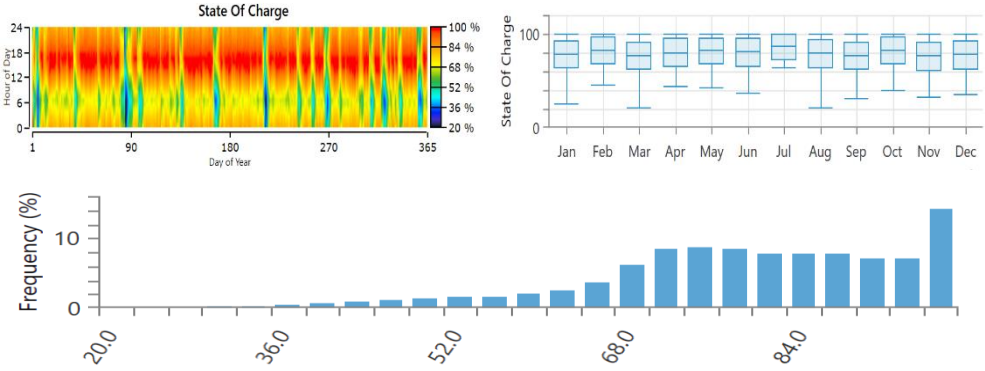


Figure 6: FESS SoC and Frequency for IL

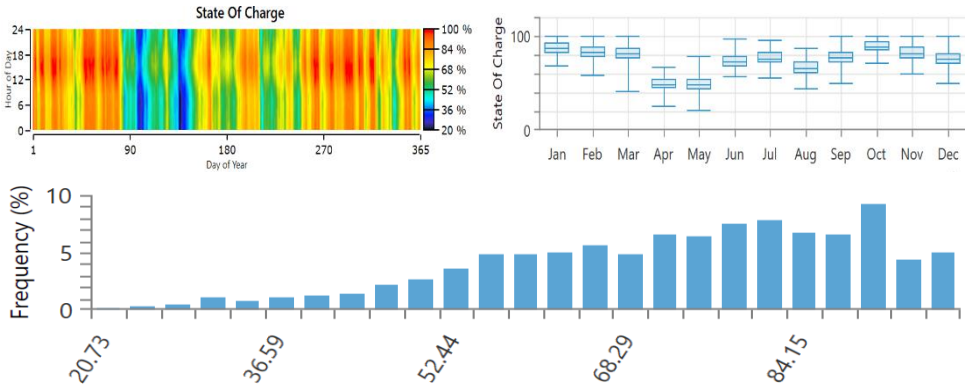


Figure 7: LIESS SoC and Frequency for ComL

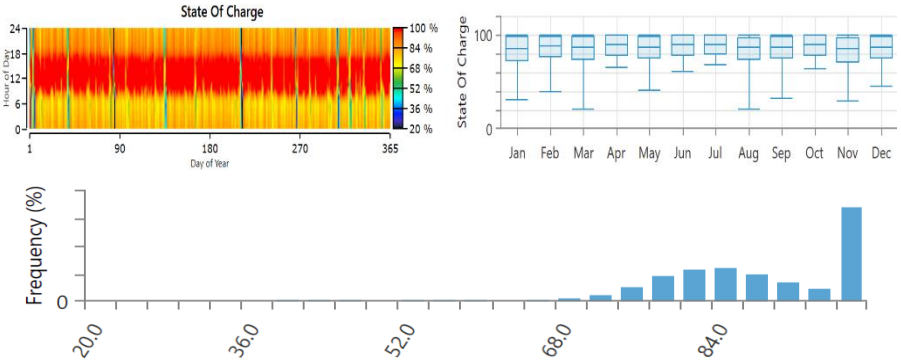


Figure 8: LIESS SoC and Frequency for CL

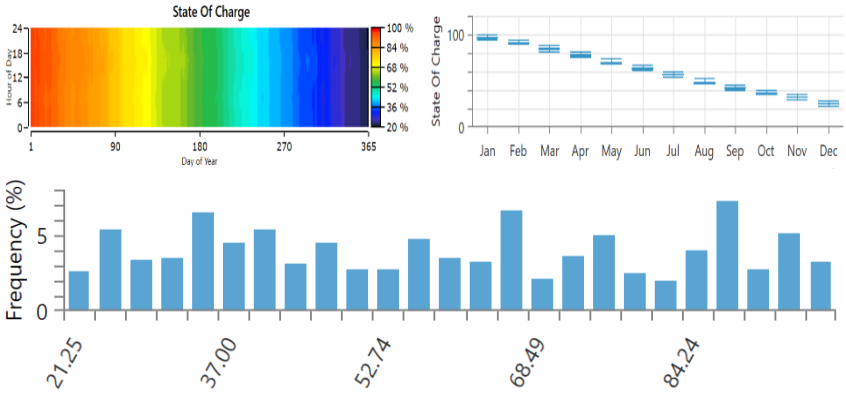


Figure 9: LIESS SoC and Frequency for RL

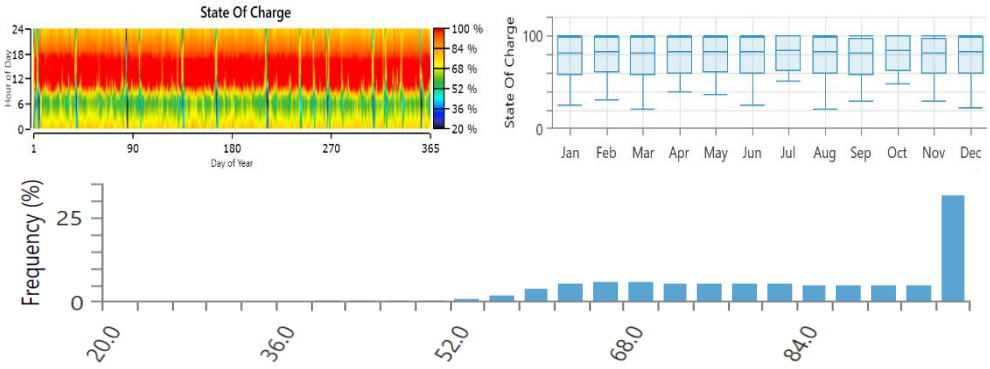


Figure 10: LIESS SoC and Frequency for IL

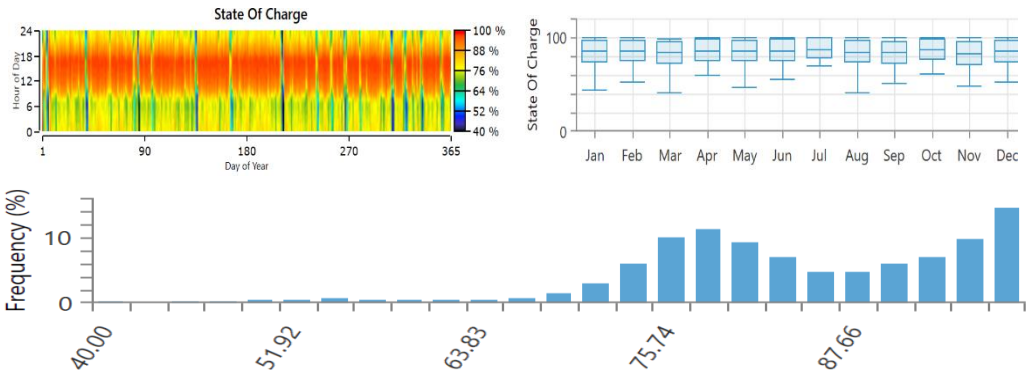


Figure 11: LAESS SoC and Frequency for ComL

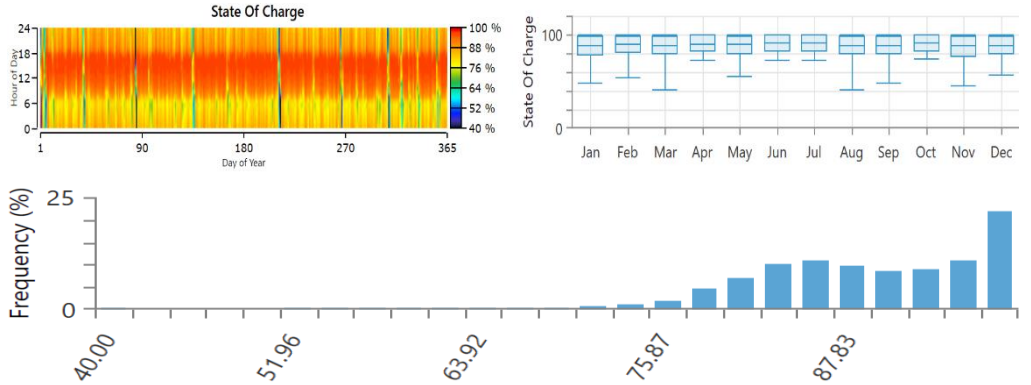


Figure 12: LAESS SoC and Frequency for CL

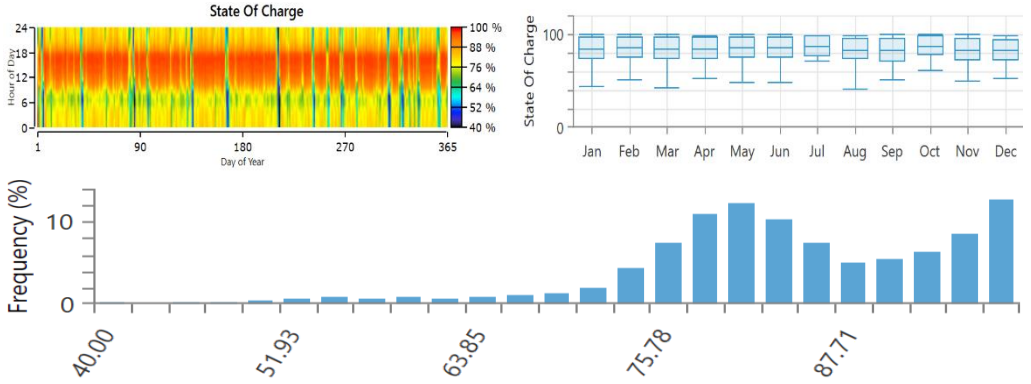


Figure 13: LAESS SoC and Frequency for RL

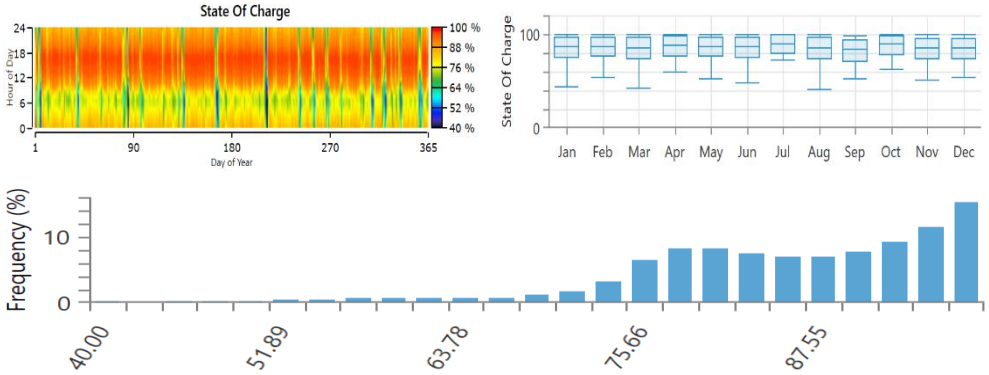


Figure 14: LAESS SoC and Frequency for IL

3.2 Technical Performance Analysis

The technical performance of FESS, LIESS, and LAESS under RL, CL, IL, and ComL profiles is presented in Table 4. The results revealed that there is a significant variations across ESS and load profiles. It was observed from Table 4 that FESS possessed the lowest SD of 5.38 kWh/yr under RL while the highest SD of 10,117 kWh/yr was reported for LAESS under IL. It can be inferred from the various ESS loading that IL generally results in high SD. Similarly, the lowest Losses of 233 kWh/yr was obtained for LIESS under RL while the highest of 1,247,935 kWh/yr was obtained for LAESS under IL. It can be generally observed that RL results in lowest Losses whereas IL results in high Losses for all the ESS loading. The reported values of AT showed that the lowest of 2,519 kWh/yr was found in FESS under RL while highest of 5,586,275 kWh/yr was found in LAESS under IL. In the same manner, it can be generally observed that RL exhibits lowest AT whereas IL results in high AT for various ESS loading. It can be seen from the USC reported in Table 4 that the lowest of 18.6 kWh was recorded for LAESS under RL while the highest of 41,751 kWh was recorded for LAESS under IL. Note also that an examination of the USC across all the ESS under all loading revealed that RL generally exhibited lowest USC while IL exhibited highest USC across all ESS. Interestingly, it was found that FESS and LIESS possessed the same CSL of 15 yr across all loading conditions while LAESS exhibited varying CSL where the lowest of 9,62 yr was recorded under ComL. In a similar manner, Auto has the same 0 $/kWh for FESS for all loading conditions while LIESS and LAESS exhibited varying Auto ranging from 22.5 $/kWh in LAESS under CL to 1,705 $/kWh LIESS under RL. Finally, it can be seen that FESS and LIESS have the same SWC value of 0.005 $/kWh and 0.246 $/kWh, respectively, for all the loads. The highest SWC value of 0.6288 $/kWh was observed in LAESS under ComL.

Arising from the analysis presented thus far, it can be generally concluded that load type generally impacts the technical performance of ESS. Also, except for RL and IL that demonstrated consistent trends across all ESS in terms of Losses, AT, and USC, other load exhibited inconsistent trend across the ESS.

Table 4. Summary of FESS, LIESS, and LAESS under RL, CL, IL, and ComL profiles

Storage Type	Load	SD kWh/yr	Losses kWh/yr	AT kWh/yr	USC kWh	CSL Yr	Auto $/kWh	SWC $/kWh
FESS	RL	5.38	563	2,519	19.3	15	0	0.005
	CL	749	69,051	309,203	5,163	15	0	0.005
	IL	9,847	1,229,531	5,503,826	40,563	15	0	0.005
	ComL	81.9	7351	32,917	191	15	0	0.005
LIESS	RL	788	233	2,614	800	15	1,705	0.246
	CL	512	26,807	254,581	2400	15	23.8	0.246
	IL	7490	542,524	5,150,682	28,800	15	28.8	0.246
	ComL	252	3,725	35,467	800	15	116	0.246
LAESS	RL	6.43	566	2,535	18.6	9.78	39.7	0.419
	CL	571	58,487	261,862	2,274	10	22.5	0.419
	IL	10,117	1,247,935	5,586,275	41,751	9.96	41.8	0.419
	ComL	94.7	7,743	34,677	250	9.62	36.3	0.6288

Note. SD = Storage Depletion; AT = Annual Throughput; USC = Usable Storage Capacity; CSL = Cycle Service Life; Auto = Autonomy; SWC = Storage Wear Cost.

3.3 Economic Performance Analysis

The comparative economic performance indicators for all the ESS under different load profiles is presented in Table 5. It can be seen from the Table 5 that the lowest BC, CC, and TSC, of $18,221.23, $ 901.89, and $32,318.56, respectively, was recorded for FESS-RL as well as the lowest PVC of $5,809.17 and LCOE of $0.5263 for LIESS-RL and FESS-CL, respectively. Similarly, the highest BC and TSC of $45,891,655.32 and $72,907,772.98, respectively, was recorded for LAESS-IL while the highest PVC of $33,588,030.98, highest CC of 1,915,464.78, and highest LCOE of $20.28 for LIESS-IL, FESS-IL, and LIESS-RL, respectively. Generally, LAESS had relatively constant LCOE values ranging from RL to ComL Interestingly, the most capital-intensive configuration LIESS at the same scale as LAESS recorded a lower PVC than LAESS under CL. A case-wise loading assessment of all the ESS indicates that industrial-scale systems consistently incurred the highest economic costs, a direct consequence of the substantially larger storage capacity and energy throughput required at industrial scale. It can be concluded from this analysis that ESS cost on a per kWh basis depends on the load characteristics and size which justifies the need to align ESS choice to load.

4. CONCLUSION

In this study, a comprehensive comparative analysis of three ESS namely; FESS, LIESS, and LAESS under RL, CL, IL, and ComL conditions were presented. The study leveraged HOMER Pro simulation tool to model the ESS under the four load conditions. In total, 12 simulations scenarios were presented and analysed to determine the most viable ESS for the various load. The most viable ESS was determined using operational,

technical, and economic performance analysis based on metrics like LCOE, USC, Auto, SD, TSC, SoC, and frequency.

Table 5: Comparative economic performance of FESS, LIESS, and LAESS under different load profiles

Storage Type	Load	BC ($)	PVC ($)	CC ($)	TSC ($)	LCOE ($)
FESS	RL	18,221.23	13,195.44	901.89	32,318.56	0.6085
	CL	3,668,056.75	2,166,963.20	183,218.51	6,018,238.46	0.5263
	IL	28,970,047.36	30,782,779.20	1,915,464.78	61,668,291.34	0.5449
	ComL	199,219.64	349,167.74	8,335.41	556,722.79	0.7112
LIESS	RL	1,070,370.01	5,809.17	757.59	1,076,936.78	20.28
	CL	3,211,110.04	3,399,771.04	168,206.47	6,779,087.55	0.5931
	IL	38,533,320.52	33,588,030.98	770,393.59	72,891,745.10	0.6440
	ComL	1,070,370.01	106,034.47	10,433.68	1,186,838.17	1.52
LAESS	RL	20,675.15	12,376.26	1,098.29	34,149.69	0.6432
	CL	2,493,257.70	3,859,327.46	151,008.66	6,503,593.83	0.5690
	IL	45,891,655.32	26,116,297.74	899,819.92	72,907,772.98	0.6443
	ComL	280,817.02	200,861.25	8,892.92	490,571.18	0.6288

Note. BC = Battery Cost; PVC = Present Value Cost; CC = Capital Cost; TSC = Total System Cost; LCOE = Levelized Cost of Energy.

Operationally, it can be concluded that LIESS generally possessed a good and predictable SoC performance for all load profiles with the highest cycling under IL and significant SoC variability under RL. It is concluded from the technical analysis that RL and IL demonstrated consistent trends across all ESS in terms of Losses, AT, and USC while CL and ComL exhibited inconsistent trend across the ESS. Economically, it can be concluded from the twelve load scenarios that industrial-scale systems consistently incurred the highest economic costs. This is attributed to substantially larger storage capacity and energy throughput required at industrial scale. It can be concluded from the economic analysis that ESS cost on a per kWh basis depends on the load characteristics and size. It can be generally concluded that load type generally impacts the operational, technical, and economic performance of the selected ESS. This study finds application in the renewable energy industry as a guide for appropriate selection of ESS considering the load characteristics. Future studies will explore the possibility of deploying artificial intelligence (AI) models for optimal ESS selection.

REFERENCES

[1] T. Ahmad and D. Zhang, "A critical review of comparative global historical energy consumption and future demand : The story told so far," *Energy Reports*, vol. 6, pp. 1973–1991, 2020, doi: 10.1016/j.egyr.2020.07.020.

[2] M. Ram *et al.*, "Global energy transition to 100 % renewables by 2050 : Not fi ction , but much needed impetus for developing economies to leapfrog into a sustainable future," *Energy*, vol. 246, p. 123419, 2022, doi: 10.1016/j.energy.2022.123419.

[3] A. O. Amole, A. O. Tafa, and O. A. Bamido, "Assessment of solar-powered projects ' functionality and failures in selected remote locations of southwestern Nigeria," *Soc. Impacts*, vol. 7, no. October 2025, p. 100171, 2026, doi: 10.1016/j.socimp.2026.100171.

[4] E. H. Sepúlveda-oviedo, "Impact of environmental factors on photovoltaic system performance degradation," *Energy Strateg. Rev.*, vol. 59, no. January, p. 101682, 2025, doi: 10.1016/j.esr.2025.101682.

[5] A. Hassan, J. Ahmed, S. Papadopoulos, F. Kahwash, and K. Goh, "A comprehensive review of frequency response and control strategies for grid-connected solar photovoltaic systems," *Renew. Sustain. Energy Rev.*, vol. 226, no. PC, p. 116324, 2026, doi: 10.1016/j.rser.2025.116324.

[6] A. O. Amole, R. A. Owosibo, O. B. Adewuyi, S. Oladipo, and N. O. Imarhiagbe, "Comparative analysis

of control strategies for solar photovoltaic/diesel power system for stand-alone applications," *Renew. Energy*, p. 119717, 2023, doi: 10.1016/j.renene.2023.119717.

[7] T. Khatib, "A review of battery energy storage system for renewable energy penetration in electrical power system : Environmental impact , sizing methods , market features , and policy frameworks," vol. 7, no. June, 2025.

[8] P. Stanchev and N. Hinov, "Comparative Techno-Economic and Life Cycle Assessment of Stationary Energy Storage Systems : Lithium-Ion , Lead-Acid , and Hydrogen," pp. 1–29, 2025.

[9] D. A. Elalfy, E. Gouda, M. Fawzi, V. Bure, and B. E. Sedhom, "Comprehensive review of energy storage systems technologies , objectives , challenges , and future trends," vol. 54, no. June, 2024, doi: 10.1016/j.esr.2024.101482.

[10] K. Ricin *et al.*, "Lithium-ion batteries and the future of sustainable energy : A comprehensive review," *Renew. Sustain. Energy Rev.*, vol. 223, no. June, p. 115971, 2025, doi: 10.1016/j.rser.2025.115971.

[11] C. Borerwe and O. M. Longe, "Techno-economic analysis of large-scale battery energy storage system for stationary applications in South Africa Techno-economic analysis of large-scale battery energy storage system for stationary applications in South Africa".

[12] M. M. Hasan, R. Haque, M. I. Jahirul, M. G. Rasul, I. M. R. Fattah, and N. M. S. Hassan, "Advancing energy storage : The future trajectory of lithium-ion battery technologies," *J. Energy Storage*, vol. 120, no. April, p. 116511, 2025, doi: 10.1016/j.est.2025.116511.

[13] A. Alsharif *et al.*, "Journal of Insights in Basic and Applied Sciences Energy Systems Corresponding author : Alsharifutm@gmail.com," vol. 2, no. 1, pp. 154–171, 2026.

[14] P. Parvizi, M. Jalilian, A. M. Amidi, M. R. Zangeneh, and J. Riba, "From Present Innovations to Future Potential : The Promising Journey of Lithium-Ion Batteries," 2025.

[15] X. Liu, W. Li, X. Guo, B. Su, S. Guo, and Y. Jing, "Advancements in Energy-Storage Technologies : A Review of Current Developments and Applications," no. April 2024, pp. 1–39, 2025.

[16] C. Hermanu, B. Apribowo, S. Sarjiya, S. P. Hadi, and F. D. Wijaya, "Optimal Planning of Battery Energy Storage Systems by Considering Battery Degradation due to Ambient Temperature : A Review , Challenges , and New Perspective," 2022.

[17] E. Ventosa *et al.*, "Redox flow batteries : Status and perspective towards sustainable stationary energy storage," vol. 481, 2021, doi: 10.1016/j.jpowsour.2020.228804.

[18] W. Sharmoukh, "RSC Advances materials , viability , and industrial applications," *RSC Adv.*, vol. 15, no. April, pp. 10106–10143, 2025, doi: 10.1039/D5RA00296F.

[19] C. Zhao, P. B. Andersen, C. Træholt, and S. Hashemi, "Grid-connected battery energy storage system : a review on application and integration," *Renew. Sustain. Energy Rev.*, vol. 182, no. May, p. 113400, 2023, doi: 10.1016/j.rser.2023.113400.

[20] G. Gkoumas, P. Foteinopoulos, I. Andreev, M. Graurov, and P. Stavropoulos, "Industrial Energy Storage System Selection : A Decision Framework and Digital Implementation Demonstrated Through a Peak-Shaving Case Study," pp. 1–37, 2026.

[21] S. Shirguppikar *et al.*, "Characterization of Li-ion battery and state of charge Estimation methods for diverse battery chemistries : a review," vol. 1, pp. 1–34, 2025.

[22] K. Stein, M. Tun, M. Matsuura, and R. Rocheleau, "Characterization of a Fast Battery Energy Storage System for Primary Frequency Response," pp. 1–12, 2018, doi: 10.3390/en11123358.

[23] S. Salisu, M. W. Mustafa, L. Olatomiwa, and O. O. Mohammed, "Assessment of technical and economic feasibility for a hybrid PV-wind-diesel-battery energy system in a remote community of north central Nigeria," *Alexandria Eng. J.*, vol. 58, no. 4, pp. 1103–1118, 2019, doi: 10.1016/j.aej.2019.09.013.

[24] J. I. Chowdhury, N. Balta-Ozkan, P. Goglio, Y. Hu, L. Varga, and L. McCabe, "Techno-environmental analysis of battery storage for grid level energy services," *Renew. Sustain. Energy Rev.*, vol. 131, no. August 2019, p. 110018, 2020, doi: 10.1016/j.rser.2020.110018.

[25] J. O. Oladigbolu, M. A. M. Ramli, and Y. A. Al-Turki, "Techno-economic and sensitivity analyses for an optimal hybrid power system which is adaptable and effective for rural electrification: A case study of Nigeria," *Sustain.*, vol. 11, no. 18, 2019, doi: 10.3390/su11184959.

[26] C. Series, "Development of an Off-Grid Solar Power System to Support a Water Filtration System Development of an Off-Grid Solar Power System to Support a Water Filtration System," pp. 0–8, 2025, doi: 10.1088/1742-6596/2942/1/012037.

[27] M. Rana, H. Mo, G. M. Shafiullah, L. Qiao, and D. Dong, "Optimal sizing of battery storage for cost-effective peak shaving in regional distribution networks," *J. Energy Storage*, vol. 141, no. PD, p. 119502, 2026, doi: 10.1016/j.est.2025.119502.

[28] Q. Wang, T. Gao, and X. Li, "SOC Estimation of Lithium-Ion Battery Based on Equivalent," pp. 1–15, 2022.

[29] P. Xu and R. Zhou, "The Methods for Estimating State of Charge in Lithium-Ion Batteries," 2026.

[30] A. O. Amole, S. Oladipo, O. E. Olabode, K. A. Makinde, and P. Gbadega, "Analysis of grid/solar

photovoltaic power generation for improved village energy supply: A case of Ikose in Oyo State Nigeria," *Renew. Energy Focus*, vol. 44, pp. 186–211, Mar. 2023, doi: 10.1016/j.ref.2023.01.002.

[31] I. E. Kosmadakis and C. Elmasides, "A Sizing Method for PV – Battery – Generator Systems for Off-Grid Applications Based on the LCOE," 2021.

[32] J. Tan *et al.*, "Electrochemically Driven Phase Transition in LiCoO 2 Cathode," pp. 1–10, 2021.

[33] P. E. Riley *et al.*, "Faster Lead-Acid Battery Simulations from Porous-Electrode Theory : Part I . Physical Model Faster Lead-Acid Battery Simulations from Porous-Electrode Theory : Part I . Physical Model," 2019, doi: 10.1149/2.0301910jes.